Eur. Phys. J. D **19**, 137–145 (2002)
DOI: 10.1140/epjd/e20020066

THE EUROPEAN PHYSICAL JOURNAL D
EDP Sciences

Magnetic guiding of cold neutral atoms using a V-shaped current-carrying conductor

N. Liu[1,2], W. Gao[2], and J. Yin[1,2,a]

[1] Department of Physics, East China Normal University, Shanghai 200062, P.R. China
[2] Department of Physics, Suzhou University, Suzhou, Jiangsu 215006, P.R. China

Received 17 November 2000 and Received in final form 26 May 2001

Abstract. A new scheme to magnetically guide cold, neutral atoms using a V-shaped current-carrying conductor is proposed. The spatial distributions of the magnetic fields, potentials and forces generated by the V-shaped current-carrying conductor are calculated, and the relationship between the magnetic field and the parameters of the V-shaped current-carrying conductor are analyzed in detail. Our study shows that the V-shaped current-carrying conductor proposed here can be used to guide cold atoms in the weak-field-seeking state, and to construct various atom-optical elements, such as atomic funnel, atomic beam-splitter and atom interferometer and so on, and even to realize a single-mode atomic waveguiding under certain conditions.

PACS. 03.75.Be atom and neutron optics – 32.80.Pj Optical cooling of atoms; trapping – 85.70.Ay Magnetic device characterization, design, and modeling

1 Introduction

The guiding and trapping of cold atoms relies on the interactions either of magnetic fields or of light fields with neutral atoms. The intensity (or polarization) gradient of light beams can provide a strong friction, which can be used to cool atoms from room temperature to $\sim$1 μK temperature, and the optical dipole forces can be used to guide and confine cold atoms. As a feasible method to realize the precise manipulations and controls of neutral atoms, two kinds of atomic guides using red- or blue-detuned laser fields were proposed [1–5] and demonstrated [6–14]. The first one is that a red-detuned Gaussian laser beam [9] or a red-detuned Gaussian mode in a hollow optical fiber (HOF) [1,6] is used to guide cold atoms, which can be called "*red-detuned laser guiding of neutral atoms*". In this scheme, the dipole force from the intense Gaussian beam or Gaussian mode will attract the guided atoms to the center of the Gaussian beam or of the Gaussian mode (that is, the center of hollow region in the HOF) where the laser intensity is the maximum, which will result in a strong heating for the guided atoms due to the both spontaneous emission and photon scattering effects. The second one is that a blue-detuned evanescent-light wave in the HOF [2,3,7,8,12–14] or a blue-detuned hollow laser beam (HLB) [4,5,10,11] is used to guide cold atoms, which can be called "*blue-detuned laser guiding of neutral atoms*". Since the dipole force from the evanescent-light wave (or from the HLB) will repel the cold atoms to the center of the HOF (or of the HLB) where the intensity is the minimum, even equals zero, then the spontaneous emission effect of the guided atoms is negligible as the detuning of the laser field is very large, but the photon scattering effect always existed. In addition, the intensity fluctuations of the laser beams will also result in a small heating of the guided atoms.

It is a challenging problem to avoid heating the atoms during the laser atomic guiding process. For this, a new atomic guiding scheme using a magnetostatic field was first proposed by Hau [15] and demonstrated by Schmiedmayer [16] experimentally. When an atom in the weak-field-seeking state moves in a magnetic field with a minimum value, it will feel a gradient force from the magnetic field and will be repulsed to the minimum of the magnetic field. In recent years, various atomic magnetic guiding schemes, such as using one, two or four current-carrying wires [17–21], or using two identical and interwound current-carrying solenoids [22], even using an ac Ioffe tube [23], have been proposed and demonstrated. Since it is difficult to alter the magnetic fields from permanent magnets, whereas the magnetic fields generated by current-carrying wires can be easily changed, both theoretical and experimental studies on the magnetic manipulations and controls of cold, neutral atoms using current-carrying wires have obtained fast development [24], and a new field as called "integrated atom optics" has being formed.

In this paper, we propose a novel and simple method to guide cold, neutral atoms using a static magnetic field, which is generated by a V-shaped current-carrying conductor (V-CCC). This V-CCC can produce a suitable

[a] e-mail: jpyin@suda.edu.cn

$$B_x = \Bigg[\frac{I}{2a}\sin\theta\Bigg(2|-z-x\cot\theta|\Bigg(\arctan\Bigg(\frac{x+z\cot\theta}{|-z+x\cot\theta|}\Bigg)-\arctan\Bigg(\frac{x+z\cot\theta-2a\csc\theta}{|-z+x\cot\theta|}\Bigg)\Bigg)\csc\theta(x\cos\theta-z\sin\theta)$$
$$+|-z+x\cot\theta|\Bigg(|-z-x\cot\theta|\cot\theta\Bigg(-2\ln|x^2+z^2|+\ln|(z-2a\cos\theta)^2+(x-2a\sin\theta)^2|+\ln|(z-2a\cos\theta)^2+(x+2a\sin\theta)^2|\Bigg)$$
$$-2\Bigg(\arctan\frac{-x+z\cot\theta}{|-z-x\cot\theta|}+\arctan\frac{x-z\cot\theta+2a\csc\theta}{|-z-x\cot\theta|}\Bigg)\csc\theta(x\cos\theta+z\sin\theta)\Bigg)\Bigg)\mu_0\Bigg]\Big/(4\pi|-z-x\cot\theta||-z+x\cot\theta|) \quad (1)$$

and

$$B_z = \Bigg[\frac{I}{2a}\sin\theta\left(2|-z-x\cot\theta|\left(\arctan\left(\frac{x+z\cot\theta}{|-z+x\cot\theta|}\right)-\arctan\left(\frac{x+z\cot\theta-2a\csc\theta}{|-z+x\cot\theta|}\right)\right)\cot\theta\csc\theta(x\cos\theta-z\sin\theta)\right.$$
$$+|-z+x\cot\theta|\left(|-z-x\cot\theta|\left(-\ln\left|(z-2a\cos\theta)^2+(x-2a\sin\theta)^2\right|+\ln\left|(z-2a\cos\theta)^2+(x+2a\sin\theta)^2\right|\right)\right.$$
$$\left.\left.+2\left(\arctan\frac{-x+z\cot\theta}{|-z-x\cot\theta|}+\arctan\frac{x-z\cot\theta+2a\csc\theta}{|-z-x\cot\theta|}\right)\cot\theta\csc\theta(x\cos\theta+z\sin\theta)\right)\right)\mu_0\Bigg]\Big/(4\pi|-z-x\cot\theta||-z+x\cot\theta|) \quad (2)$$

magnetic field gradient to transversely confine cold atoms and balance the action of the gravity field on the atoms. Our study shows that such a magnetic guide will be very useful in the experiments of atom optics and can be used to construct various atom-optical elements, such as atomic funnel, atomic beam-splitter, and atom interferometer, and so on. In Section 2, the equations to calculate the magnetic field from a V-shaped current-carrying conductor are derived. In Section 3, we calculate the spatial distribution of the magnetic field generated by the V-CCC and analyze the relations between the magnetic field (including magnetic potential and force) and the parameters of the V-CCC. In Section 4, the potential applications of the V-CCC in atom optics are briefly discussed. The main results and conclusions are summarized in the last section.

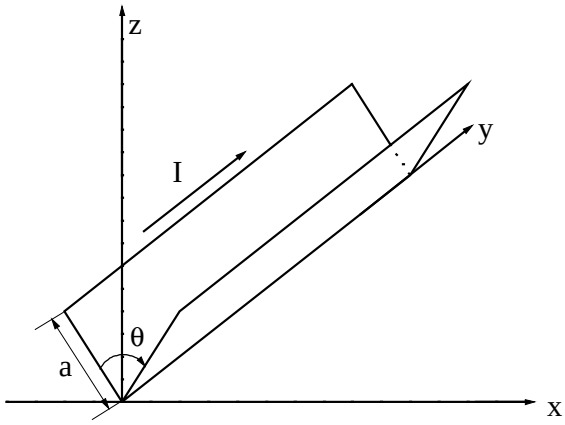

Fig. 1. Schematic diagram of atomic magnetic guiding using a V-shaped current carrying conductor (V-CCC) with a current I, an angle θ and a side width a.

2 Derivation of formulas

Though the derivation of formulas to calculate the magnetic field from a V-shaped current-carrying conductor is tedious, it can be obtained from the usual elementary calculation based on Ampere's circuit law. Let us consider a V-shaped current-carrying conductor (V-CCC) as shown in Figure 1, and assuming that it is infinitely long in the y-direction, according to the Ampere's circuit law, the x and z components of the magnetic field generated by the V-CCC are given by, respectively:

see equations (1, 2) above

then we have

$$|B(x,z)| = \sqrt{B_x^2(x,z)+B_z^2(x,z)}, \quad (3)$$

where I is the current in the V-CCC, a and θ are the side width and the angle between two sides of the V-shaped conductor, respectively. From equations (1–3), we can calculate the spatial distribution of the magnetic field $|B|$ from the V-CCC, and analyze the relationship between the B field and the parameters of the V-CCC. The corresponding potential or the gradient force for cold atoms can also be calculated and analyzed from the above equations, respectively.

Considering the interaction of an atom (with a magnetic dipole moment μ) with a static, inhomogeneous magnetic field B, the trapping potential for cold atoms, due to Zeeman effect, is a position dependent and given by

$$U_{\rm Mag} = -\boldsymbol{\mu}\cdot\mathbf{B} = g_{\rm F}\, m\mu_{\rm B}B, \quad (4)$$

where m is the magnetic quantum number, $g_{\rm F}$ is the Lande g-factor, and $\mu_{\rm B}$ is the Bohr magneton. When $\boldsymbol{\mu}\cdot\mathbf{B} > 0$, the potential is attractive, and the atoms in the strong-field-seeking state will be attracted to the maximum of magnetic field, which can be used to guide the strong-field-seeking atoms along the current-carrying wire [16]. While $\boldsymbol{\mu}\cdot\mathbf{B} < 0$, the potential is repulsive, and the atoms in the weak-field-seeking state will be repulsed to the minimum of magnetic field (such as the position ($x = 0$,

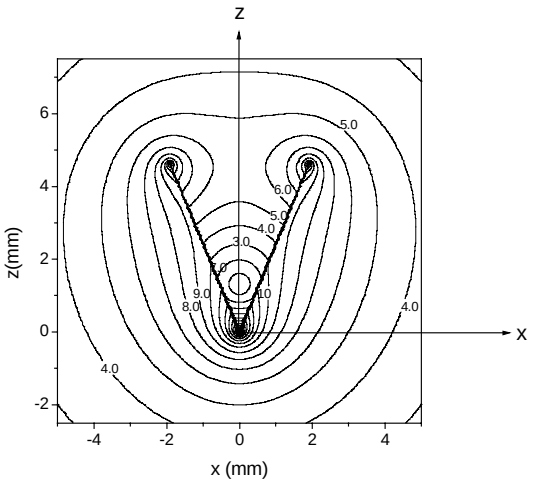

Fig. 2. The contours ($x-z$-plane) of the magnetic field $|B|$ generated by the V-CCC for $\theta = 45°$, $a = 5$ mm, and $I = 10$ A. The corresponding magnetic field values are shown in contours.

$z_0 \approx 1\,300$ μm) in Figure 2 is a field minimum), which can be used to guide (or trap) the weak-field-seeking atoms [17–20,25]. For ^{87}Rb atoms in the $|F = 2, m = 2\rangle$ state, the trapping potential is given by

$$U_{\rm Mag} = 67.2|B| \qquad (\mu{\rm K}). \tag{5}$$

In equation (5), the unit of magnetic field B is Gauss.

To ensure the projection of the atomic angular momentum onto the magnetic field direction, m remains constant during the interaction of atom with the magnetic field, we should assume that the motion of guided cold atoms in the magnetic field B must satisfy the condition of adiabatic approximation. That is, when the atom moves in the magnetic field, it will not make transit between energy levels, and the internal state of the atom changes continuously following the magnetic field at the location of the atoms. From equation (4), the gradient force of the magnetic field on the cold atoms is given by

$$\mathbf{F} = -\boldsymbol{\nabla} U_{\rm Mag} = -m g_{\rm F}\, \mu_{\rm B} \boldsymbol{\nabla} B. \tag{6}$$

Obviously, when $mg_{\rm F} > 0$, the moving, weak-field-seeking atoms will be repelled to the minimum of the magnetic field by the repulsive gradient force F.

3 Theoretical calculations and analysis

According to equations (1–3), the contours of magnetic field $|B|$ generated by the V-CCC in Figure 1 was calculated, and the result is shown in Figure 2. It is clear from Figure 2 that there is a point of zero magnetic field at the z-axis, and its coordinate position is at $(0, z_0)$, which is like a magnetic tube with a point of $B = 0$ at the position $(0, z_0)$ and can be used to guide cold atoms in the weak-field-seeking state along the y-direction. It is well-known that near the point of zero magnetic field, the guided atoms may be lost by Majorana transitions. So to eliminate this atomic loss, we can add a small bias field B_0 along the guiding axis (*i.e.*, the y-direction) to provide a quantized axis for the guided atoms.

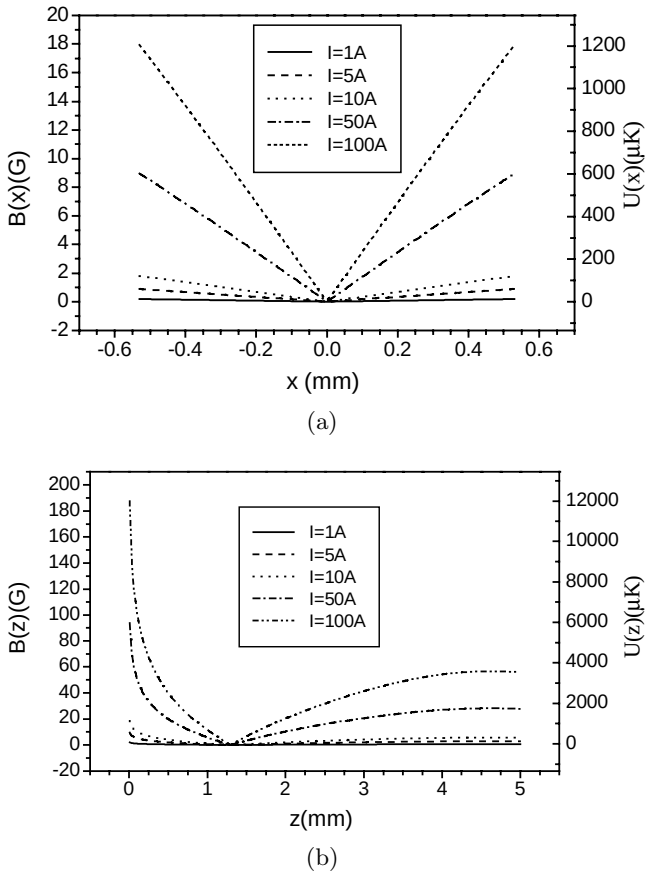

Fig. 3. The relationship between the current I in the V-CCC and the distribution of the magnetic field, (a) $B(x)$ at $z = z_0$ and (b) $B(z)$ at $x = 0$, for $\theta = 45°$, $a = 5$ mm, and $I =$ 1 A, 5 A, 10 A, 25 A, 50 A and 100 A. The right vertical axis represents the corresponding magnetic potential for ^{87}Rb atoms.

We investigated the relationship between the distribution of the magnetic field ($B(x)|_{z=z_0}$ or $B(z)|_{x=0}$) and the parameters (I, θ and a) of the V-CCC, and obtained some interesting results. The relationship between the corresponding potential for ^{87}Rb atoms ($U(x)|_{z=z_0}$ or $U(z)|_{x=0}$) and the parameters of the V-CCC are also studied. Here, $B(x)|_{z=z_0}$ and $U(x)|_{z=z_0}$ are the distribution of the magnetic field B and its potential U for ^{87}Rb atoms along the x-direction when $z = z_0$, whereas $B(z)|_{x=0}$ and $U(z)|_{x=0}$ are that along the z-direction when $x = 0$. Next, we will show our calculated results and the corresponding theoretical analysis.

First, the relationship between the magnetic field B and the current I in the V-CCC is shown in Figure 3. It can be seen from Figure 3a that the magnetic field $B(x)$ at $z = z_0$ is linearly changed with the x-coordinate (like a quadrupole field), and the magnetic field and its

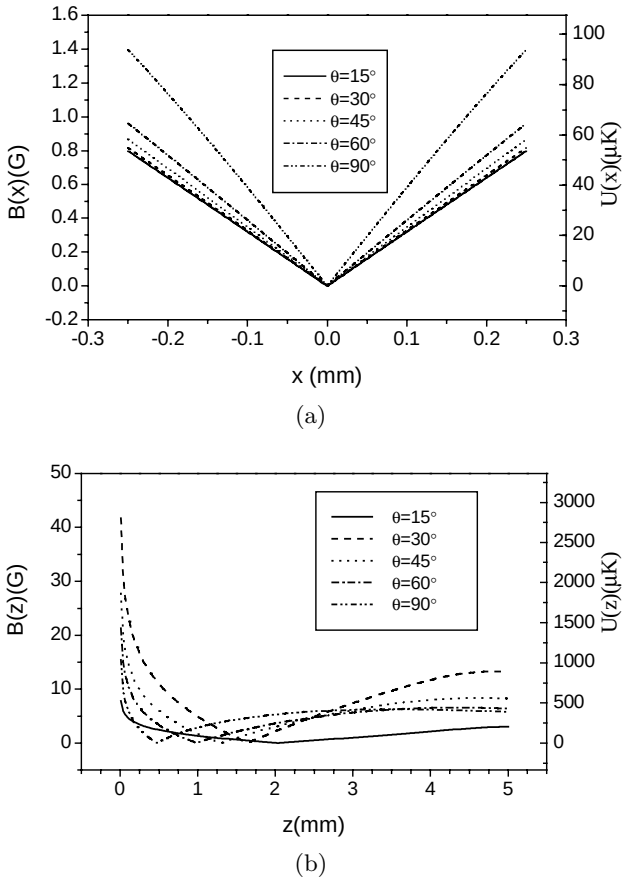

Fig. 4. The relationship between the opening angle θ of the V-shaped conductor and the distribution of the magnetic field, (a) $B(x)$ at $z = z_0$ and (b) $B(z)$ at $x = 0$, for $I = 10$ A, $a = 5$ mm, and $\theta = 15°$, $30°$, $45°$, $60°$, $90°$. The right vertical axis is the corresponding potential for ^{87}Rb atoms.

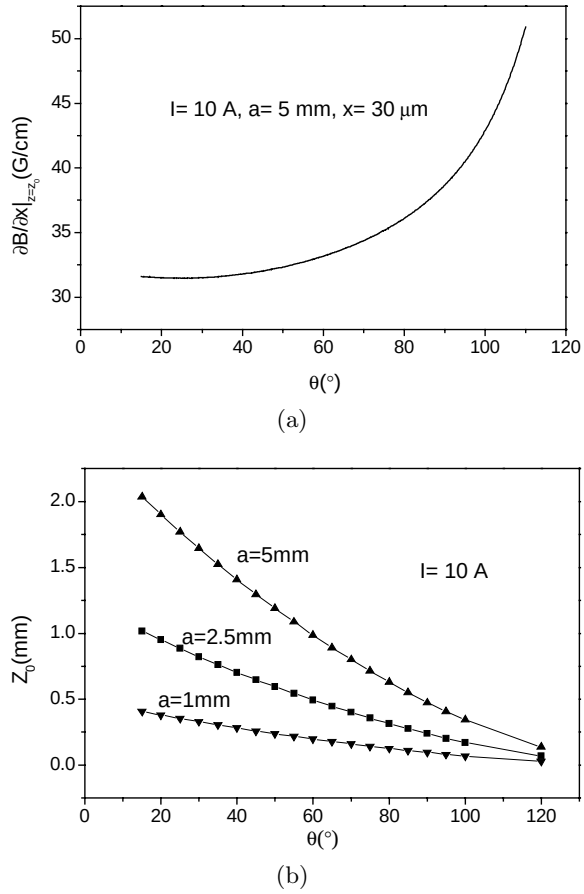

Fig. 5. (a) The relationship between the B-field gradient in the x-direction and the angle θ, and (b) the relationship between the position z_0 of zero B-field point and the angle θ when $I = 10$ A and $a = 5$ mm.

gradient will be reached to the maximum at two walls of the V-CCC, whereas Figure 3b shows that

(1) there is a point of the zero magnetic field at the position z_0,
(2) the magnetic field $B(z)$ at $x = 0$ is nonlinearly changed with the z-coordinate,
(3) and the gradient of the magnetic field $B(z)$ below the z_0 point is far larger than that the z_0 point mentioned above.

When $a = 5$ mm, $\theta = 45°$, and $I \geq 50$ A, we obtain $B(x)_{\max} \geq 9$ G and $B(z)_{\max} \gg B(x)_{\max}$, the corresponding potential $U(x)_{\max} = 600$ μK, which is high enough to collect and transversely confine cold atoms from a standard magneto-optical trap (MOT) with a temperature of 120 μK. Here $B(x)_{\max}$ is the maximum of $B(x)$ near two walls of the V-CCC at $z = z_0$, whereas $U(x)_{\max}$ is the corresponding maximal potential. Moreover, when $a = 5$ mm, $\theta = 45°$, the position $(0, z_0)$ of zero B-field is about at (0, 1.3 mm), which is not related to the current I.

Secondly, Figure 4 shows the relations between the magnetic field B and the angle θ. We can see from Figure 4a that the bigger the angle θ is, the larger the gradient of the magnetic field $B(x)$ is, and their relationship is shown in Figure 5a. Whereas Figure 4b shows that the position $(0, z_0)$ of zero B-field will be lowered with the increase of the angle θ, and their relationship is shown in Figure 5b and it can be described by

$$z_0 \approx A_1 + A_2\, \mathrm{e}^{-(\theta-\theta_0)/w} \quad (\mu\mathrm{m}), \tag{7}$$

where A_1, A_2, θ_0 and w are four fitting parameters, which is related to the side width a. When $a = 5$ mm, we obtain $A_1 \approx -1\,026.3$, $A_2 \approx 3\,073.03$, $\theta_0 \approx 15°$ and $w \approx 105.78$. From Figure 4, moreover, when $a = 5$ mm, $I = 10$ A, and $\theta \geq 30°$, we have $B(x)_{\max} \geq 10$ G, and $U(x)_{\max} \geq 0.67$ mK, and the point of zero B-field is dropped to 0.12 mm from 2.1 mm as the angle θ is increased from 15° to 120°.

Finally, the relationship between the side width a and the magnetic field, $B(x)$ at $z = z_0$ or $B(z)$ at $x = 0$, was studied, the results are shown in Figure 6. It is obvious from Figure 6 that the smaller the side width a is, the larger the gradient of the B-field is, and the point of zero B-field is risen as the increase of the width a, and their

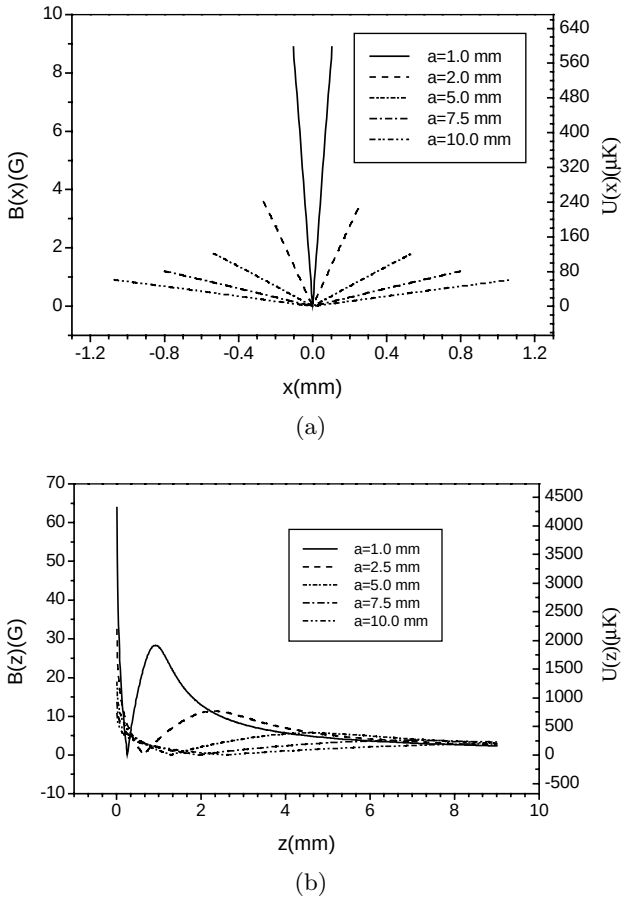

Fig. 6. The relationship between the side width a of the V-shaped conductor and the distribution of the magnetic field, (a) $B(x)$ at $z = z_0$ and (b) $B(z)$ at $x = 0$, for $I = 10$ A, $\theta = 45°$, and $a = 1$ mm, 2.5 mm, 5 mm, and 10 mm. The right vertical axis shows the corresponding potential for ^{87}Rb atoms.

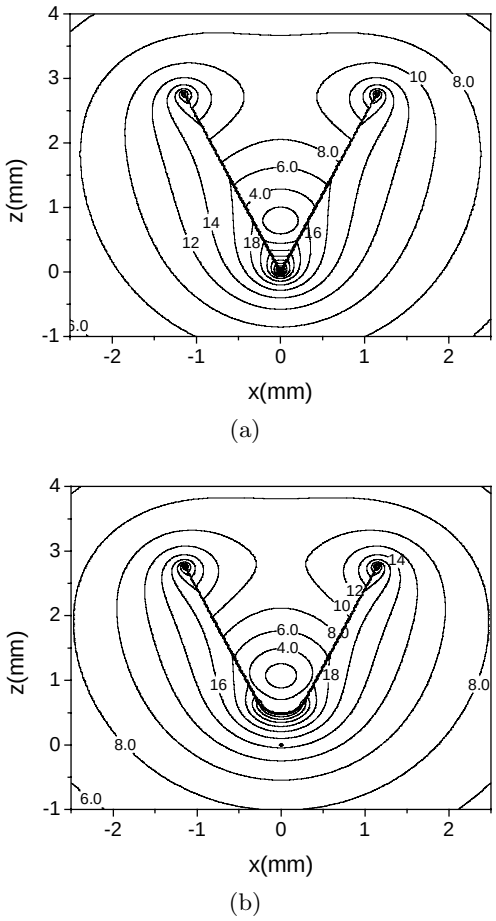

Fig. 7. The contours ($x-z$-plane) of the magnetic field generated by the V-CCC (a) without and (b) with a finite radius ($r = 0.3$ mm) of curvature in the bending point of the V-shaped conductor for $\theta = 45°$, $a = 3$ mm, and $I = 10$ A. The corresponding magnetic field values (in Gauss) are shown in contours.

relationship can be approximated by

$$z_0 \approx k(\vartheta)a, \tag{8}$$

where the coefficient k is a constant for a given θ-value. When $I = 10$ A, $\theta = 45°$, and $a = 1$ mm, we obtain $B(x)_{\max} \approx 9$ G and the corresponding potential $U(x)_{\max}$ is $\sim$600 μK, and the point of zero B-field is gone up from 0.28 mm to 2.5 mm when the width a is increased from 1 mm to 10 mm, and the corresponding coefficient $k \approx 0.259$.

In combination of equation (7) with equation (8), we have a general equation to describe the relationship between the position (z_0) of zero B-field point and the parameters (a and θ) of the V-CCC as follows

$$z_0 \approx \left(A_1 + A_2\, \mathrm{e}^{-(\theta-\theta_0)/w}\right) a. \tag{9}$$

From Figures 3b, 4b and 6b, we found that there are two maximum points of the $B(z)$, one is at the bottom of the V-CCC, and another is above the zero point z_0 of the magnetic field. When $I \geq 25$ A, $\theta \geq 30°$, and $a \leq 5$ mm, we have $B(z)_{\max} \geq 15$ G and $U(z)_{\max} \geq 1$ mK, which is far higher than the maximal gravity potential of ^{87}Rb atoms in the magnetic guiding tube formed by the V-CCC. This shows that even if the V-CCC as shown in Figure 1 is inverted horizontally, it can also be used to guide cold atoms along the y-direction in the gravity field.

Similarly, we also studied the relationships between two components (F_x, F_z) of the gradient force of the magnetic field B and the parameters (I, θ and a) of the V-CCC, and found that the larger the current I is, or the bigger the angle θ, the smaller the side width a is, the stronger the B-field gradient force is. When $\theta = 45°$, $a = 5$ mm, $I = 50$ A and above the point z_0 of zero B-field, we obtained $F_{z_{\max}} \geq 2 \times 10^{-22}$ N, which is about l00 times of the gravity force exerted on ^{87}Rb atom. This shows that F_z is strong enough to counteract the action of the gravity force on the guided atoms. Moreover, due to imperfect manufacture of the V-shaped conductor, there may be a finite radius of curvature in the bending point

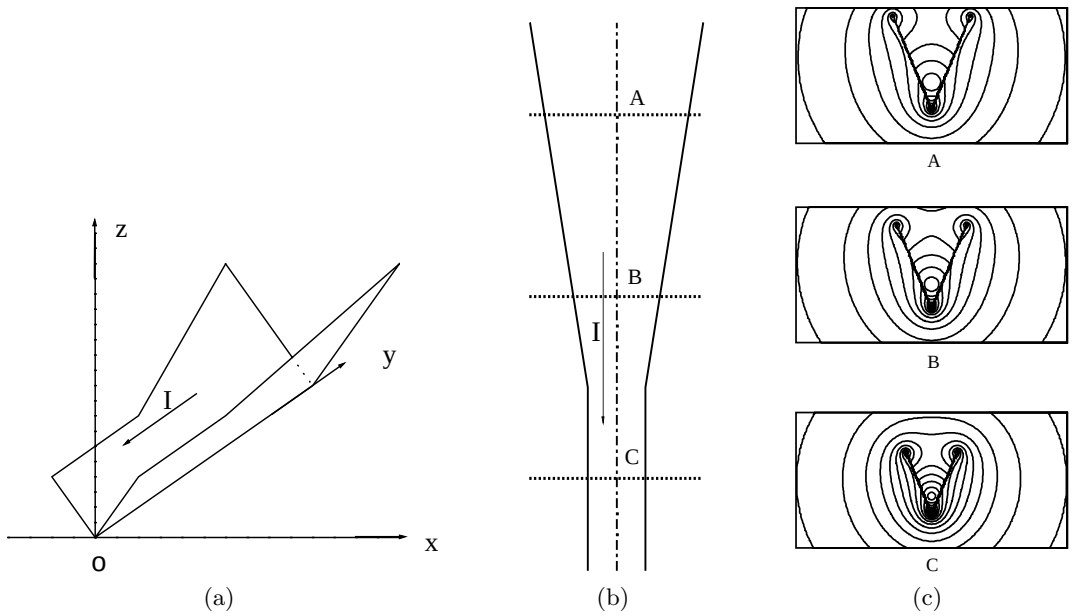

Fig. 8. (a) The scheme of atom funnel formed by the VCCC (3D view). (b) and (c) Layout (2D vertical view) and the magnetic field or potential for an atom funnel. Contours are drawn at 1 Gauss intervals and the first contour shows 1 Gauss.

of the V-shaped conductor. We studied the influence of such a finite radius of curvature on the magnetic guiding properties, and the calculated results are shown in Figure 7. Comparing Figure 7a with Figure 7b, we can find that a finite radius of curvature in the bending point of the V-shaped conductor only results in the elevation of magnetic guiding center $(0, z_0)$ along the z-axis and slight increase of magnetic-field gradient, but this doesn't affect other magnetic guiding properties of cold atoms.

From the above analysis, we know that when the current I is higher, the angle θ is bigger, and the side width a is smaller, the transverse confinement for the cold atoms will be more tight, then the averaged diameter (*i.e.*, the mean transverse moving range) of the guided cold atoms in the magnetic tube generated by the V-CCC will become very small. In particular, when this diameter is close to the mean wavelength of de Broglie wavelength $\lambda = \sqrt{2\pi\hbar^2/(mkT)}$ of cold atoms, it seems possible to realize a single-mode atomic waveguiding. So under the certain conditions, the V-CCC can be used to realize single-mode atomic waveguiding. For example, when $I \geq 50$ A, $\theta \geq 30°$, and $a = 1$ mm, the diameter of a potential contour with $\sim$20 μK is smaller than 1 μm, this shows that a single-mode waveguiding for the cold atoms with a temperature of lower than 20 μK may be realized under the above conditions. Moreover, the gradient of the magnetic field in the x-direction is smaller than that in the z-direction, so in the analysis on the interaction of the guided atoms with the magnetic field B, we only need in fact to consider the distribution of the magnetic field, trapping potential and the dipole force in the x-direction, *i.e.*, ones only need to consider $B(x)$, $U(x)$ and $F_x = \partial B/\partial x|_{z=z_0}$.

4 Applications of V-CCC

Atomic funnel, or atomic beam-splitter, or atom interferometer and so on, are one of the basic atom-optical elements (or devices), and they have wide and important applications in the experiments with cold atoms or cold atomic beam. So the design of various atom-optical elements is one of very interesting subjects in atom optics. In this section, we will discuss the potential applications of the V-CCC in atom optics and give some interesting and practical atom optical elements.

4.1 Atomic funnel

From Figures 4 and 5, the V-CCC with a fixed angle θ and a linearly increased width a along the y-direction can be used to form an atomic funnel, which is shown in Figure 8. In which, (a) and (b) are the three-dimensional (3D) view and 2D vertical view of atomic funnel respectively, and (c) is the corresponding B-field contours or atomic funnel potentials. It is clear from Figure 8c that when the side width a of V-CCC is linearly decreased, the radius of the magnetic-field contour with an identical Gaussian value will also be reduced. This shows that the guiding potentials have different modes in atomic funnel and it is possible to realize the transformation of atomic waveguiding mode from a multimode state to a single-mode one in our funnel when the part of the V-CCC below the cross-section (C) satisfies the conditions of single-mode waveguiding.

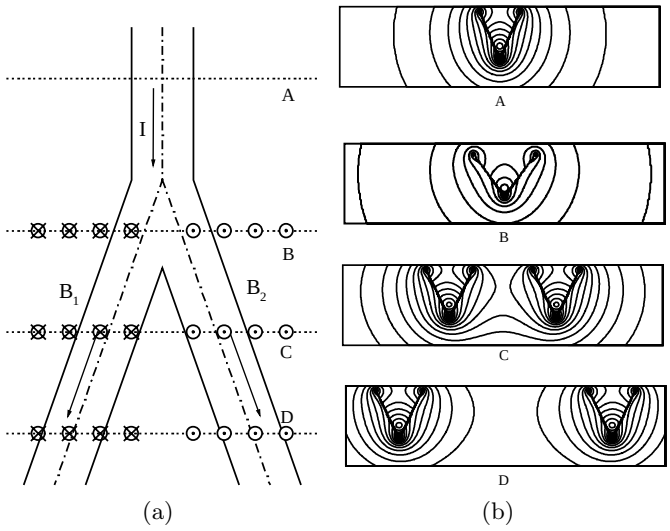

Fig. 9. (a) VCCC layout and (b) the magnetic field or potential for a Y-shaped beam splitter using a VCCC. In which, $\mathbf{B}_1$ and $\mathbf{B}_2$, are two additional bias fields and setting $\mathbf{B}_1 = -\mathbf{B}_2$. Contours are every l Gauss (beginning at 1 Gauss).

4.2 Atomic beam-splitter

The simplest atomic beam-splitter (ABS) is a Y-shaped one with one input arm and two output arms, which can be constructed by a Y-shaped V-CCC and two bias fields with an equal but opposite directional B-field (*i.e.*, $\mathbf{B}_1 = -\mathbf{B}_2$) orthogonal to the $x-y$-plane (see Fig. 9). If without two bias fields, the points of the zero magnetic fields in two output guiding arms will be shifted to the center of the Y-shaped ABS respectively and may be close to two middle conductor-walls of Y-shaped V-CCC due to the superposing each other of two magnetic fields generated by the currents (I_1, I_2, and $I_1 = I_2 = I/2$) in two output arms of the Y-beam splitter. Therefore, we have to add two inverse bias fields ($\mathbf{B}_1 = -\mathbf{B}_2$) near the splitting range of the Y-shaped ABS so as to shift two points of the zero B-fields back to their self center of two output arms in the Y-shaped ABS, respectively. Of course, when two output arms of the Y-beam splitter are separated to be large enough, this Y-beam splitter will give two independent output guides and no need to add two inverse bias fields ($\mathbf{B}_1 = -\mathbf{B}_2$).

It is clear from Figure 9B that when a current I is sent to an input arm of the Y-beam splitter, the atoms will be guided in this arm and the atomic wave function can be split after the splitting point of the Y-beam splitting potential, and the atoms are guided in both output arms, respectively. Moreover, the Y-shaped beam splitting potential is completely symmetric with respect to its input guide, so it can be used to realize coherent splitting for many waveguiding modes, which is similar to the case of two-wire Y-beam splitter [25].

Similarly, by using two Y-beam splitters, an X-shaped beam splitter with two incoming channels and two outgoing channels will be formed, which is shown in Figure 10.

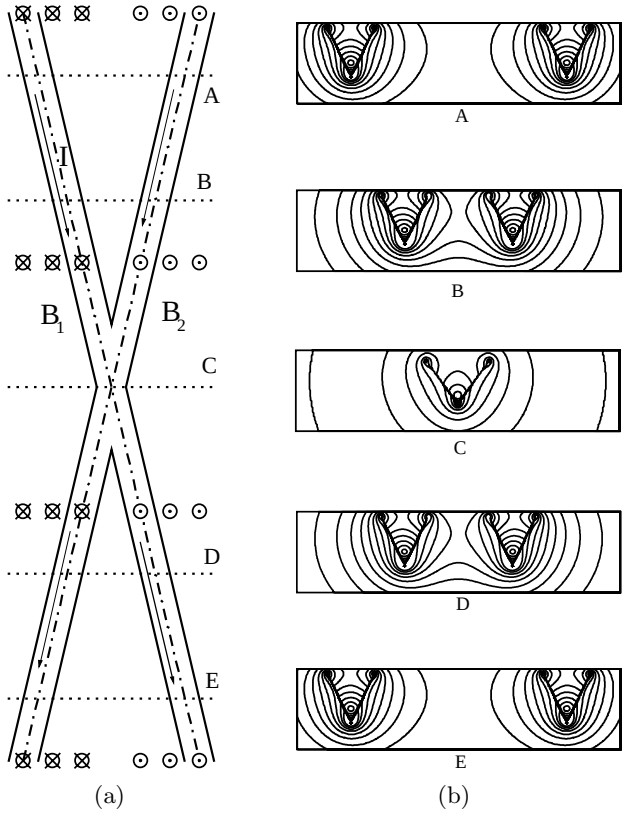

Fig. 10. (a) VCCC layout and (b) the magnetic field or potential for an X-shaped beam splitter. Where the meaning of $\mathbf{B}_1$, $\mathbf{B}_2$, and their relationship are the same as that in Figure 9. Contours are drawn at 1 Gauss intervals and the first contour shows 1 Gauss.

The symmetry of the Y-beam splitter with respect to the incoming guide is broken and it will be much harder to obtain coherent splitting for many waveguiding modes at the same time, which is similar to the case of two-wire X-beam splitter [25].

4.3 Atom interferometer

When two Y-shaped beam splitters with coherent splitting as shown in Figure 8 are connected by mouth to mouth of two Y-shaped forks, an atom interferometer will be set up (see Fig. 11). It is clear from Figure 11b that two Y-beam splitting potential are completely symmetric and can ensure coherent splitting at the first splitting point and coherent superposition at the second splitting point, and coherent propagation between two splitting points (in two guiding channels) for many waveguiding modes. So this configuration gives a superposition of atomic internal states and can be applied in many experiments on atomic interferometry, particularly in single-mode atom interference.

Next, we will briefly discuss the possible loading of cold atoms from an atomic beam (or a standard MOT) into our V-CCC. From the above analysis and discussion,

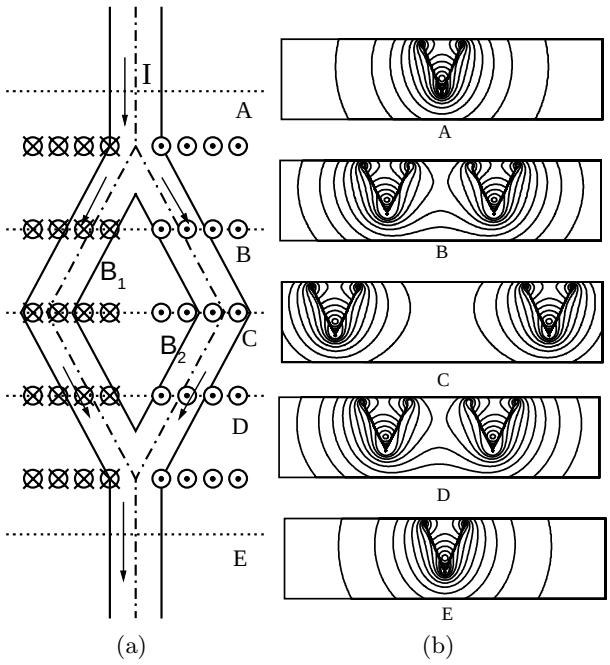

Fig. 11. (a) VCCC layout and (b) the magnetic field or potential for an atom interferometer. In which, the meaning of $\mathbf{B}_1$, $\mathbf{B}_2$, and their relationship are the same as that in Figure 9. Contours are every 1 Gauss (beginning at 1 Gauss).

to choose a current I (due to heating effect) as small as possible and obtain a higher transversely-trapped potential for the guided atoms, the side width a of V-shaped conductor should be a value as smaller as possible. In particular, in order to realize a single-mode atomic waveguide, the side width a must be smaller than 1 mm. In this case, an atomic optical funnel with a dark hollow beam [26] or an atomic magnetic funnel with the V-shaped CCC as shown in Figure 8 can be used to load cold atoms from an atomic beam (or a standard MOT) into the V-shaped CCC, and then our V-shaped guide will be realized. When the V-CCC is placed along the horizontal direction, we can use a cold atomic beam and an atomic funnel to load our V-shaped guide, whereas as the V-CCC is placed along the vertical direction, a standard MOT above the top of the V-shaped conductor can be used to load cold atoms from the MOT into our V-shape guide passing through an atomic funnel under the action of the gravity field. Moreover, because the heating effect of current in the conductor is rather serious when $I = 10 \sim 100$ A, it is necessary to cool the conductor by using semiconductor cooler or water cooling (in this case, the used conductor should be a hollow V-shaped one and the cycled cool water will be flowed in the hollow region of this special V-shaped conductor).

5 Conclusions

We have proposed a novel atomic guiding scheme based on the interaction of a magnetic dipole moment of the guided atom with a magnetic field generated by a V-shaped current carrying conductor (V-CCC). We have calculated the contours of $|B|$ field, the transverse trapping potential and force for the guided ^{87}Rb atoms, and analyzed the relationships between the resulting magnetic field (including the potential and force) and the parameters of the V-CCC, and found that there is a point of the zero magnetic field at the z-axis, and the magnetic field will be increased rapidly as the position $r(x, z)$ is away from the zero point $(0, z_0)$ of the magnetic field, which is like a magnetic tube with an axis of zero B-field along the y-direction, and then guided cold atoms will be reflected by magnetic mirror effects from the tube. So our V-CCC can be used to guide cold atoms along the conductor direction, and to realize single-mode atomic waveguiding under certain conditions.

Our magnetic guide for neutral atoms is different from the wire guide and has some interesting characteristics, such as the position of the zero magnetic field in the guide using the V-shaped CCC only depend on the V-angle θ and the side length a of the conductor, and its B-field gradient is tuned with the angle θ and side length a. In particular, to form an atomic funnel, only a V-shaped CCC is needed, whereas as using wire guide, two current-carrying wires are needed at least. So our V-CCC can be conveniently used to form various atom optical elements, such as atomic funnel, Y- or X-shaped beam splitters, and atom interferometer. In addition, some other shaped current-carrying conductors, such as U-shaped, semicircle-shaped or W-shaped and so on, can be used to realize single- or double-channel atomic guiding.

This work is supported by the Natural Science Foundation of China (Grant No. 69878019 and 19834060) and the Natural Science Foundation of Jiangsu Province (Grant No. DK97139) and the Natural Science Foundation of Education Department, Jiangsu Province (Grant No. 00KJB140001) and the Fostering Foundation of New-century Academic Leader from the Educational Department of Jiangsu Province.

References

1. M.A. Ol'shanii, Yu.B. Ovchinnikov, V.S. Letokhov, Opt. Commun. **98**, 77 (1993).
2. S. Marksteiner, C.M. Savage, P. Zoller, S.L. Rolston, Phys. Rev. A **50**, 2680 (1994).
3. H. Ito, K. Sakaki, T. Nakata, W. Jhe, M. Ohtsu, Opt. Commun. **115**, 57 (1995).
4. Jianping Yin, Yifu Zhu, Wenbao Wang, Yuzhu Wang, W. Jhe, J. Opt. Soc. Am. B **15**, 25 (1998).
5. Jianping Yin, Yifu Zhu, W. Jhe, Yuzhu Wang, Phys. Rev. A **58**, 509 (1998).
6. M.J. Renn, D. Montgomery, O. Vdovin, D.Z. Anderson, C.E. Wieman, E.A. Comell, Phys. Rev. Lett. **75**, 3253 (1995).
7. M.J. Renn, E.A. Donley, E.A. Comell, C.E. Wieman, D.Z. Anderson, Phys. Rev. A **53**, R648 (1996).
8. M.J. Renn, A.Z. Zozulya, E.A. Donley, E.A. Comell, D.Z. Anderson, Phys. Rev. A **55**, 3684 (1997).
9. L. Pruvost *et al.*, Opt. Commun. **166**, 199 (1999).

10. Jianping Yin, Yueming Lin, K. Lee, H. Nha, H. Noh, Yuzhu Wang, K. Oh, U. Paek, W. Jhe, J. Kore. Phys. Soc. **33**, 362 (1998).
11. Xinye Xu, V.G. Minogin, K. Lee, Yuzhu Wang, W. Jhe, Phys. Rev. A **60**, 4796 (1999).
12. H. Ito, T. Nakata, K. Sakaki, M. Ohtsu, K.I. Lee, W. Jhe, Phys. Rev. Lett. **76**, 4500 (1996).
13. R.G. Dall *et al.*, J. Opt. B **1**, 396 (1999).
14. H. Ito, K. Sakaki, M. Ohtsu, W. Jhe, Appl. Phys. Lett. **70**, 2496 (1997).
15. L.V. Hau, J.A. Golovchenko, M.M. Bums, Phys. Rev. Lett. **74**, 3138 (1995).
16. J. Schrniedmayer, Phys. Rev. A **52**, R13 (1995).
17. J. Denschlag, D. Cassettari, J. Schmiedmayer, Phys. Rev. Lett. **82**, 2014 (1999).
18. D. Muller D.Z. Anderson, R.J. Grow, P.D.D. Schwindt, E.A. Cornell, Phys. Rev. Lett. **83**, 5194 (1999).
19. N.H. Deforer, C.S. Lee, V. Lorent, J.H. Thywissen, M. Dmdic, P.M. Westervelt, M. Prentiss, Phys. Rev. Lett. **84**, 1124 (2000).
20. M. Key, I.G. Hughes, W. Rooijakkers, B.E. Sauer, E.A. Hinds, Phys. Rev. Lett. **84**, 1371 (2000).
21. J. Fortagh, H. Ott, A. Grossmann, C. Zimmermann, Appl. Phys. B **70**, 701 (2000).
22. J.A. Richmond, S.N. Chormaic, B.P. Cantwell, G.I. Opat, Acta Phys. Slov. **48**, 481 (1998).
23. Lifang Xu, Jianping Yin, Yuzhu Wang, Opt. Commun. **188**, 93 (2000).
24. D. Cassettar, A. Chenet, R. Folman, A. Haase, B. Hessmo, P. driger, T. Maier, S. Schneider, T. Calarco, J. Schmiedmayer, Appl. Phys. B **70**, 721 (2000).
25. V.I. Balykin, Adv. At. Mol. Opt. Phys. **4**, 181 (1999).